

The Experimental and Analytical Investigation of the Flexural Capacity of Pre-Cast Composite Beams

H.J. Ko, W.K. Hong, S.C. Park, G.T. Lim and J.H. Kim
Department of Architectural Engineering
Kyung Hee University, Yongin, Korea

Abstract

This paper describes pre-cast composite beams with reverse T type steels embedded at the ends. Concrete is cast in place to form slabs. The experimental and analytical investigations of flexural capacity of the composite beams with reverse T type steels at each end are performed to understand the behaviour of the composite beams. The strain-compatibility approach proposed by AISC (American Institute of Steel Construction) is used for the analysis of the composite beams. In this method, one correct location of a neutral axis is determined from one of the equilibrium equations set up for each neutral axis. The equation that satisfies the equilibrium of the composite section determines the correct location of the neutral axis. Both test and calculated values of the flexural capacity based on a strain-compatibility approach at the maximum load limit state are well correlated, demonstrating that the analytical method provides a practical approach for predicting the behaviour of composite beams.

Keywords: pre-cast composite beam, strain compatibility, flexural moment.

1 Introduction

A composite structure is optimized to utilize the strengths of both steel and concrete. Unlike other structures composed of a single material, the composite structure is greatly improved by rigidity, which enables it to provide structural stability. The composite beam used in the study is a Steel Framed Reinforced Concrete Structure (SRC) type, which is a widely used composite structure. Reverse T type steels are embedded in the precast concrete and the concrete is cast in place to form slabs, which connect the joints of beams and columns.

A strain-compatibility approach that allows accurate prediction of beam behaviour is adopted in order to analyze the flexural capacity of precast composite beams. The

AISC (American Institute of Steel Construction) proposes the strain-compatibility approach as an analytical method for composite beams. This paper is written based on the strain-compatibility approach proposed by the AISC. The strain-compatibility approach assumes the stress state of components generated at each limit state to set an equilibrium equation, and determines the location of a neutral axis that exists in the cross-section [1, 2].

This paper is intended to assess the flexural capacity of each end of the composite beams that are embedded in the reverse T type steels. To do so, the flexural capacity of each end is calculated based on a design created using the strain-compatibility approach. It is compared with experimental data for the same ends [1 - 5].

2 Strain Compatibility Analysis

2.1 Definition of the limit state

It is not easy to determine the neutral axis of composite beams which consist of several different kinds of members in a cross-section. The strain-compatibility analysis approach is adopted to calculate the neutral axis and flexural capacity more accurately.

Strain compatibility analysis is a method to predict the behaviour of composite members by linearizing the strain of the SRC composite beam. This step is followed by determining the strain compatibility of the compressed concrete upper section and the assumed neutral axis. The equilibrium equation with a proportional expression is the equation for the neutral axis, which can be applied to calculate the neutral axis value [6].

When applying the strain compatibility analysis, the behaviours of SRC composite beams can be defined and classified into 4 different limit states. The ‘pre-yield limit state’ is one in which low tension reinforcement has not yet reached the yield-strain ratio. The ‘yield limit state’ is one in which lower tension reinforcement has reached the yield-strain ratio. The ‘maximum load limit state’ is one in which an upper concrete strain ratio reaches the maximum strain ratio of 0.003. The ‘failure limit state’ is one in which all different components, including concrete and steel, are removed, leaving only the steel frame to achieve perfect plasticity. Beam members are destructed. Table 1 shows the definition of each limit state in accordance with the reinforced concrete strength design.

Limit State	Definition
Pre-yield limit state	Load state in which tension reinforcement has not yet reached the yield-strain ratio ($\varepsilon_y = f_y/E_s$) of the reinforcement
Yield limit state	Load state in which tension reinforcement has reached the yield-strain ratio ($\varepsilon_y = f_y/E_s$) of the reinforcement
Maximum load limit state	Load state in which the upper compressive concrete section reached the maximum concrete strain ratio of 0.003
Failure limit state	Load state in which all different components including concrete and steel are removed, leaving only the steel frame to reach perfect plasticity. Beam members are destructed.

Table 1: Definition of the limit state

2.2 Compressive Concrete Strain Blocks

Compressive Concrete Strain Blocks are expressed as a linear function and a quadratic function based on the Kent and Park's yield-strain curve as shown in Figure 1. The integral is applied to calculate the compressive force loaded to concrete. Kent and Park suggested Eq. (1) for calculating the concrete loaded compressive force. The stress factor (α) included in Eq. (2) represents the area ratio of concrete strain blocks [7].

$$C_c = \alpha f'_c bkd \quad (1)$$

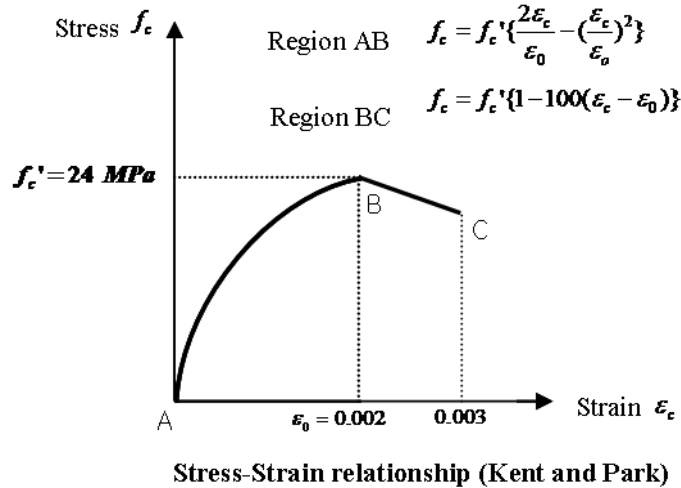


Figure 1: Stress-Strain relationship (Kent and Park)

Equation (2) represents the Stress factor, α formula.

$$\alpha = \frac{\int_0^{\varepsilon_{cm}} f_c d\varepsilon_c}{f'_c \varepsilon_{cm}} \quad (2)$$

In addition, Kent and Park proposed the centroid factor, which shows the center of a concrete strain block as demonstrated in Figure 2, in order to calculate the bending moment loaded to the concrete. (3) represents the γ formula.

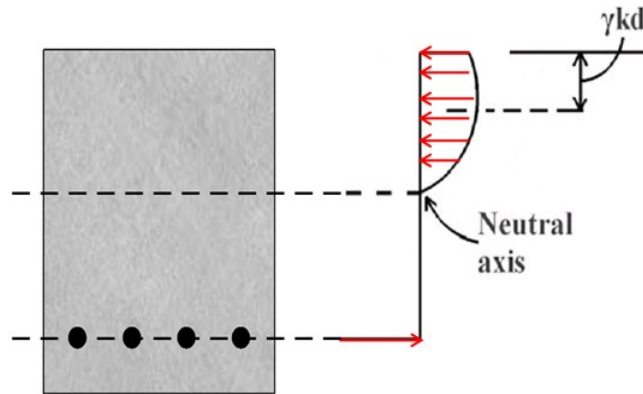


Figure 2: Centroid Factor, γ (Kent and Park)

$$\gamma = 1 - \frac{\int_0^{\varepsilon_{cm}} \varepsilon_c f_c d\varepsilon_c}{\varepsilon_{cm} \int_0^{\varepsilon_{cm}} f_c d\varepsilon_c} \quad (3)$$

3 Experiment and Analysis

3.1 Specimen of section

Figure 3 shows the cross-section of a test specimen. The concrete compressive strength of the specimen is 27 MPa, the tensile strength of a steel frame is 330MPa and the tensile strength of rebar is 400MPa. In the case of a stirrup, reinforcement bars that are 10 mm in diameter shall be aligned at 400 mm intervals. Three reinforcement bars that are 22 mm in diameter and 6 bars that are 25 mm in diameter are arranged in the upper section. Two bars that are 25 mm in diameter are included in the lower section. The dimension of the steel frame applied is 248×199×9×14(mm), and stud bolts that are 16 mm in diameter are fastened to the lower steel frame flange at 440 mm intervals and to the web at 165 mm intervals. For experimental accuracy, two specimens with the same cross-section were manufactured to carry out the experiment.

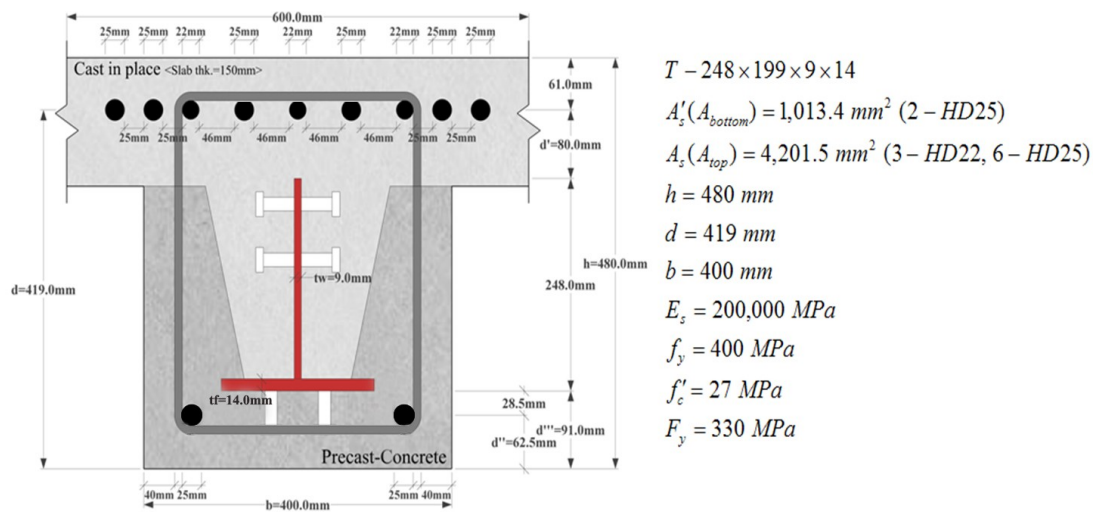


Figure 3: Detailed Cross-Section of a Specimen

A 1000 kN actuator is used for the precast composite beams produced in a factory. Simple beams are applied. The specimen span is 4500 mm and its clear span is 4000 mm. A 3 point bending method is used for the experiment in which the central part of the beams is loaded. Figure 4 shows how the load is imposed.

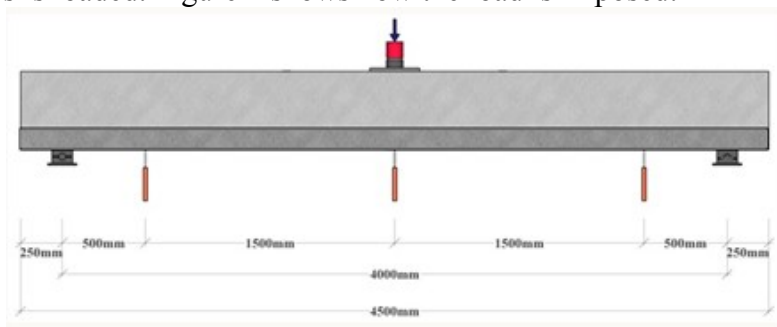


Figure 4: Loading Method

Figure 5 demonstrates the experimental scene of the precast composite beam specimen.



Figure 5: View of the Specimen Experiment

3.2 Experiment Results

Strain gauges are attached to the specimen to draw the neutral axis from specimen strain. Thirty strain gauges are installed on the steel frame, upper/lower reinforcement bars, concrete and stirrup, in order to measure the strain at various heights of the specimen cross-section.

The strain measured at each height is marked on a linear proportional graph. The point where the strain is 0 shall be the neutral axis, used to identify the location of the specimen's neutral axis. The neutral axis is drawn out under the maximum load limit status to compare the value calculated from the strain compatibility analysis. Also, the neutral axis are measured under two different conditions: when the strain gauge attached to the lower tension reinforcement reaches the yield-strain ratio and when the strain gauge attached to the upper concrete reaches the maximum strain, as determined by data analysis. Figure 6 shows a graph that expresses the strain measured as a function of the installation height of the 'specimen 1' strain gauge.

Figure 7 shows a graph that expresses the strain as a function of installation height with a 'specimen 2' strain gauge.

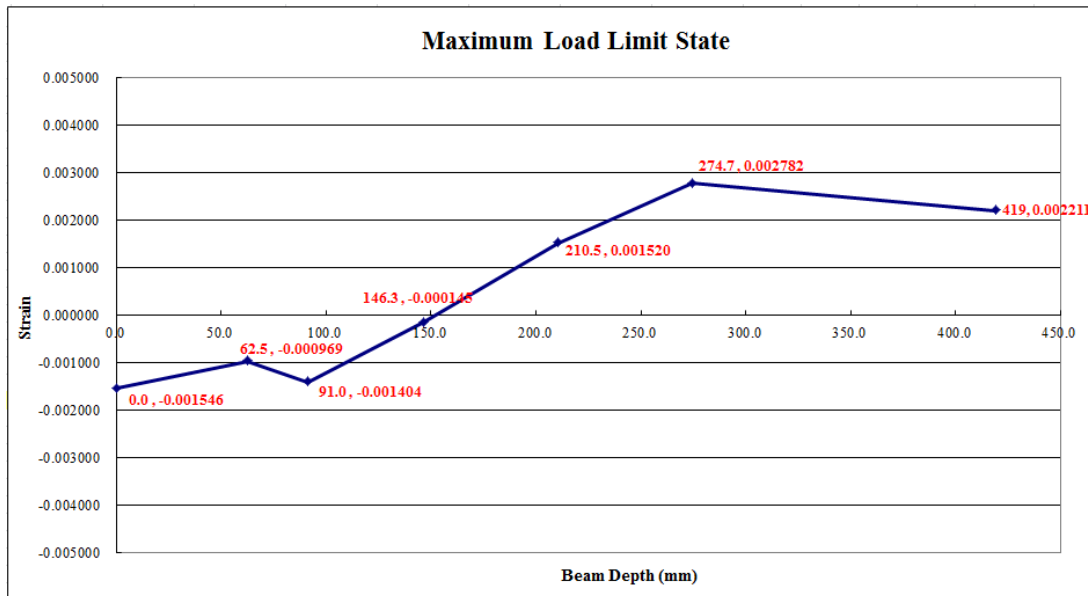


Figure 6: Transition of Strain in Maximum Load Limit State of Specimen #1



Figure 7: Transition of Strain in Maximum Load Limit State of Specimen #2

A linear interpolation method is adopted to calculate the neutral axis located between gauges. As a result of the analysis on the neutral axis, 151.89 mm is measured for Specimen 1 and 152.20 mm for Specimen 2.

3.3 Analysis Results

Figure 8 shows the cross-sections that satisfy the neutral axis location, assumed to be $CF_{ny}CW_{ny}TW_{pp}CR_{ny}TR_y$, along with the maximum load limit state, and the stress state of each member. Table 2 shows whether each component strain and assumption is met under $CF_{ny}CW_{ny}TW_{pp}CR_{ny}TR_y$.

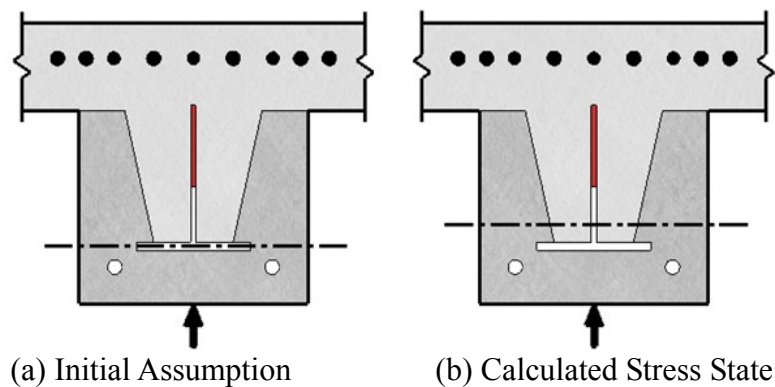


Figure 8: Maximum Load Limit State $CF_{ny}CW_{ny}TW_{pp}CR_{ny}TR_y$ Assumed Cross-Section

Location	Initial Assumption	Calculated Stress State	Strain Ratio	Assumption Satisfied or Not
Compressive Reinforcement Bar	Specific Yield	Specific Yield	0.00171808	O.K.
Upper Section of the Compressive Flange	Elasticity	Elasticity	0.00113353	O.K.
Lower Section of the Compressive Flange			0.00084638	
Lower Section of the Tension Web	Partial Plasticity	Partial Plasticity	0.00395311	O.K.
Tension Bar of the Reinforced Concrete	Yield	Yield	0.00559397	O.K.

Table 2: Comparison of the Stress States under Different Assumptions

For the assumption, $CF_{ny}CW_{ny}TW_{pp}CR_{ny}TR_y$, which fully satisfies both the assumed neutral axis location and the stress state, the strain (ϵ) value is inserted into (4) and (5) to calculate α and γ values, which are 0.761 and 0.411 respectively.

$$\alpha = \frac{\int_0^{0.002} f'_c \left\{ \frac{2\epsilon_c}{\epsilon_{co}} - \left(\frac{\epsilon_c}{\epsilon_{co}} \right)^2 \right\} d\epsilon_c + \int_{0.002}^{0.003} f'_c \{1 - 100(\epsilon_c - \epsilon_{co})\} d\epsilon_c}{f'_c \epsilon_{cm}} = 0.761 \quad (4)$$

$$\gamma = 1 - \frac{\int_0^{0.002} \epsilon_c f'_c \left\{ \frac{2\epsilon_c}{\epsilon_{co}} - \left(\frac{\epsilon_c}{\epsilon_{co}} \right)^2 \right\} d\epsilon_c + \int_{0.002}^{0.003} \epsilon_c f'_c \{1 - 100(\epsilon_c - \epsilon_{co})\} d\epsilon_c}{\epsilon_{cm} \left[\int_0^{0.002} f'_c \left\{ \frac{2\epsilon_c}{\epsilon_{co}} - \left(\frac{\epsilon_c}{\epsilon_{co}} \right)^2 \right\} d\epsilon_c + \int_{0.002}^{0.003} f'_c \{1 - 100(\epsilon_c - \epsilon_{co})\} d\epsilon_c \right]} = 0.411 \quad (5)$$

The neutral axis(c) value is calculated from (6) and (7). It is located 146.3 mm away from the lower compressive concrete section of the cross-section.

$$\begin{aligned} & \alpha f'_c b c + A'_s E_s \frac{\epsilon_c}{c} (c - d'') + A'_f E_s \frac{\epsilon_c}{c} \left(c - d''' - \frac{t_f}{2} \right) + \frac{1}{2} A'_w E_s \frac{\epsilon_c}{c} (c - d''' - t_f) \\ & = A_s f_y + A_{wp} F_y + \frac{1}{2} A_{wny} E_s \epsilon_{sy} \end{aligned}$$

$$\text{Where, } A'_w = t_w (c - d''' - t_f), A_{wp} = t_w \left\{ d - \left(c + d' + \frac{\epsilon_{sy}}{\epsilon_c} c \right) \right\}, A_{wny} = t_w \frac{\epsilon_{sy}}{\epsilon_c} c \quad (6)$$

$$\begin{aligned} & \left\{ \alpha f'_c b + \frac{1}{2} t_w \epsilon_c E_s + t_w F_y \left(1 + \frac{\epsilon_{sy}}{\epsilon_c} \right) - \frac{1}{2} t_w F_y \frac{\epsilon_{sy}}{\epsilon_c} \right\} c^2 \\ & + \{ A'_s \epsilon_c E_s + A'_f \epsilon_c E_s - t_w \epsilon_c E_s (d''' + t_f) - A_s f_y - t_w F_y (d - d') \} c \\ & + \left\{ - A'_s \epsilon_c E_s d'' - A'_f \epsilon_c E_s \left(d''' + \frac{t_f}{2} \right) + \frac{1}{2} t_w \epsilon_c E_s (d''' + t_f)^2 \right\} = 0 \end{aligned}$$

$$\therefore c = 146.3 \text{ mm} \quad (7)$$

The bending moment affecting the cross-section under $CF_{ny}CW_{ny}TW_{pp}CR_{ny}TR_y$ is calculated using Formula (8), and the value determined is 597.4 kN·m.

$$\begin{aligned}
 M_n &= \alpha f'_c b c (c - \gamma c) + A'_s E_s \frac{\varepsilon_c}{c} (c - d'')^2 \\
 &+ A'_f E_s \frac{\varepsilon_c}{c} \left\{ (c - d''' - t_f) \left(c - d''' - \frac{t_f}{2} \right) + \frac{t_f}{2} \left(c - d''' - \frac{t_f}{3} \right) \right\} \\
 &+ \frac{1}{3} A'_w E_s \frac{\varepsilon_c}{c} (c - d''' - t_f)^2 + A_s f_y (d - c) \\
 &+ \frac{1}{2} A_{wp} F_y \left(d - c - d' + \frac{\varepsilon_{sy}}{\varepsilon_c} c \right) + \frac{1}{3} A_{wny} E_s \frac{(\varepsilon_{sy})^2}{\varepsilon_c} c \\
 &= 597.4 \text{ kN} \cdot \text{m}
 \end{aligned} \tag{8}$$

$$A'_w = t_w (c - d''' - t_f), \quad A_{wp} = t_w \left\{ d - \left(c + d' + \frac{\varepsilon_{sy}}{\varepsilon_c} c \right) \right\}, \quad A_{wny} = t_w \frac{\varepsilon_{sy}}{\varepsilon_c} c$$

Figure 9 shows the strain and stress diagrams when the strain of the upper compressive concrete section reaches 0.003, the maximum load limit state, and Figure 10 demonstrates the cross-sectional yield strength.

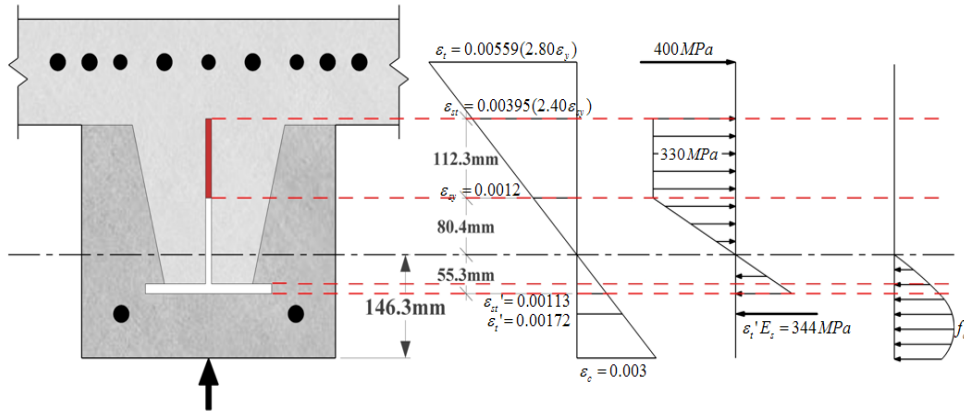


Figure 9: Strain Diagram & Stress Diagram (Maximum Load Limit State, $\varepsilon_c = 0.003$)

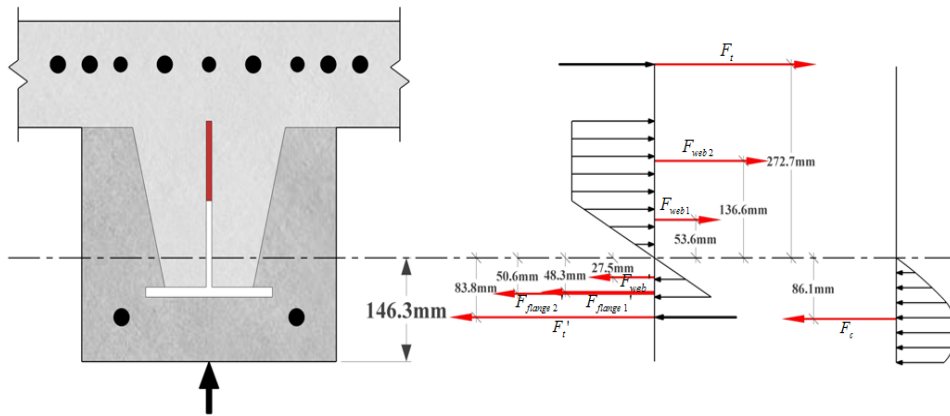


Figure 10: Cross-Sectional Yield Strength (Maximum Load Limit State, $\epsilon_c = 0.003$)

3.4 Comparative Analysis

3.4.1 Force – Strain Curve

Figure 11 and Figure 12 are the analyses of Specimen #1 and Specimen #2, which represent the force-strain relationships at the bottom reinforcement.

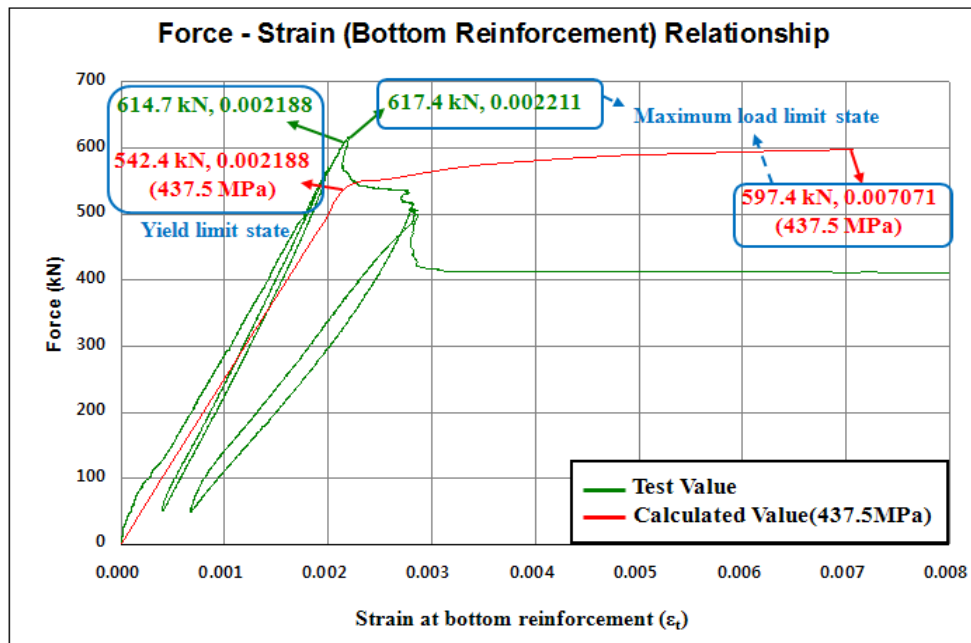


Figure 11: Force-Strain (Bottom Reinforcement) Relationship (Specimen #1)

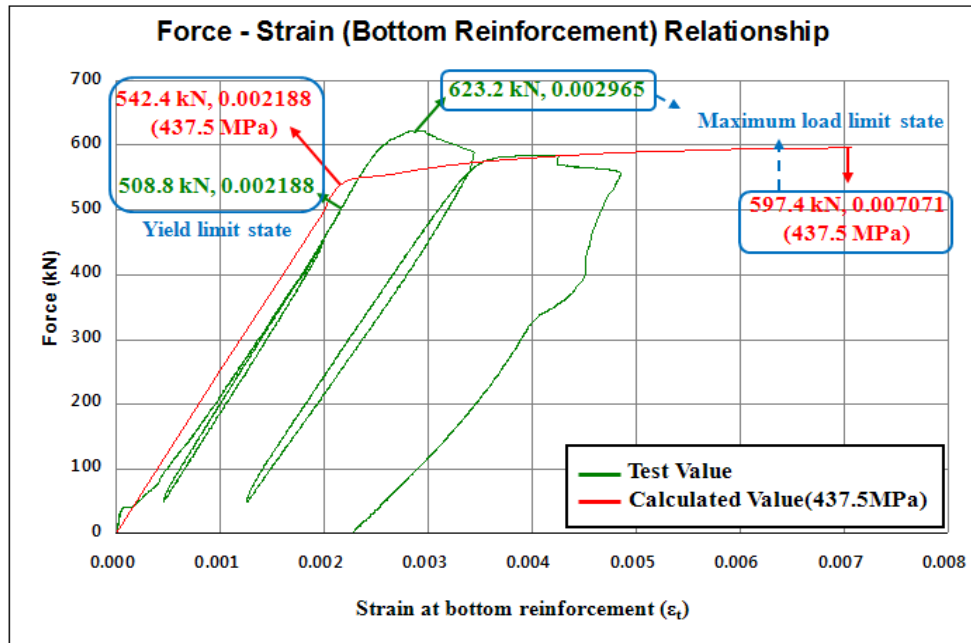


Figure 12: Force-Strain (Bottom Reinforcement) Relationship (Specimen #2)

Table 3 compares the experiment values and the analysis values for Specimen #1 and Specimen #2. Those values are compared under the maximum load limit state. The experiment value of Specimen #1 under the maximum load limit state is 617.4 kN and its analysis value is 597.4 kN. Also, the experiment value of Specimen #2 is 623.2 kN and its analysis value is 597.4 kN. As a result of analysis and comparison, the values for an inelastic area are similar.

	Specimen #1			Specimen #2		
	Experiment Value (kN)	Analysis Value (kN)	Error	Experiment Value (kN)	Analysis Value (kN)	Error
Maximum Load Limit State	617.4	597.4	20.0 (3.3%)	623.2	597.4	25.8 (4.3%)

Table 3: Comparison of Force Values between Experiment and Analysis

3.4.1 Neutral Axis

Table 4 shows the comparison of the neutral axis measured through experiment and analysis.

	Specimen #1			Specimen #2		
	Experiment Value (mm)	Analysis Value (mm)	Error	Experiment Value (mm)	Analysis Value (mm)	Error
Maximum Load Limit State	151.89	146.3	5.59 (3.7%)	152.20	146.3	5.9 (3.9%)

Table 4: Comparison of Neutral Axis between Experiment and Analysis

As a result of this comparison, the neutral axis values determined by experiment and analysis show a slight error, with not much difference between them. The error between the values is likely to be generated due to the difference in the properties of the specimen components applied during the experiment and the analysis.

In addition, when the neutral axis of the test specimen is located lower than the analysis value, it is predicted that the tensile strength of the reinforcement bar of the actual specimen will be higher than that predicted through the strain compatibility analysis.

Although there is a slight error between the analysis values and the experiment values, it is likely that the behaviour analysis based on plasticity of composite members is predictable with the strain compatibility analysis approach.

4 Result

This study compares the flexural capacity of each end as determined by the strain compatibility analysis with that of each end of the precast composite beams determined by experiment. Results are as follows:

- 1) As a result of comparing load values under the maximum load limit state, the experiment value of Specimen #1 was 617.4 kN, its analysis value was 597.4 kN and the error between those values was 20.0 kN (3.3%). The experiment value of Specimen #2 was 623.2 kN, its analysis value was 597.4 kN and the error between those values was 25.8 kN (4.3%). The result was shown to be similar.
- 2) As a result of comparing the neutral axis values under the maximum load limit state, the experiment value of Specimen #1 was 151.89 mm, its analysis value was 146.3 mm and the error between those values was 5.59 mm (3.7%). The experiment value of Specimen #2 was 152.20 mm, its analysis value was 146.3 mm and the error between those values was 5.9 mm (3.9%). The result was shown to be similar.

- 3) There is a difference between the neutral axis as determined by the experiment and that determined by the analysis due to the influence of the specimen components. Moreover, when the neutral axis of the test specimen is lower than the analysis value, the tensile strength of the reinforcement bar of the actual specimen will be higher than that predicted through strain compatibility analysis.
- 4) By applying strain compatibility analysis, the flexural capacity of pre-cast composite beam specimens was compared and analyzed. In other words the experiment values and the analysis values were compared for analysis. It is possible to predict the behaviour of composite members at the plasticity area using the strain compatibility analysis approach, and the error rate is relatively small. Therefore, it is determined that the strain compatibility analysis is highly reliable.

Acknowledgement

This work was supported by the National Research Foundation of Korea(NRF) grant funded by the Korea government(MEST) (No. 2011-0027453)."

References

- [1] W. K. Hong, S. C. Park, J. M. Kim, S. G. Lee, S. I. Kim, K. J. Yoon, H. C. Lee, "Composite beam composed of steel and pre-cast concrete (modularized hybrid system, MHS) Part I: Experimental investigation," *Struct. Des. Tall. Spec. Build.*, 19(3), 275-289, Apr. 2010.
- [2] W. K. Hong, J. M. Kim, S. C. Park, S. G. Lee, S. I. Kim, K. J. Yoon, H. C. Kim, J. T. Kim, "A new apartment construction technology with effective CO₂ emission reduction capabilities," *Energy – Int. J.*, 35(6), 2639-2646, Apr. 2010.
- [3] W. K. Hong, S. I. Kim, S. C. Park, J. M. Kim, S. G. Lee, K. J. Yoon, S. K. Kim, "Composite beam composed of steel and pre-cast concrete (modularized hybrid system, MHS) Part IV: Application for multi-residential housing," *Struct. Des. Tall. Spec. Build.*, 19(7), 707-727, Nov. 2010.
- [4] W. K. Hong, J. M. Kim, S. C. Park, S. I. Kim, S. G. Lee, H. C. Lee, K. J. Yoon, "Composite beam composed of steel and pre-cast concrete (modularized hybrid system, MHS) Part II: Analytical investigation," *Struct. Des. Tall. Spec. Build.*, 18(8), 891-905, Nov. 2009.
- [5] S. Y. Jeong, W. K. Hong, S. C. Park, G. T. Lim, E. Kim, "Investigation of the Neutral Axis in the Positive Moment Region of Composite Beams", ICECE2011, 60(87), 465-470
- [6] American Institute of Steel Construction Inc. and the Structural Steel Educational Council: Seismic Design Manual: AISC: 2006
- [7] R. Park, T. Paulay, *Reinforced Concrete Structures*. New York: JOHN WILEY&SONS, 1975.